

## PROBLEMS OF CORE CORRELATION, SEDIMENT SOURCE ASCRIPTION AND YIELD ESTIMATION IN PONSONBY TARN, WEST CUMBRIA, UK

F. OLDFIELD<sup>1\*</sup>, P. G. APPLEBY<sup>2</sup> AND K. D. VAN DER POST<sup>1</sup>

<sup>1</sup>*Department of Geography, University of Liverpool, Liverpool, L69 3BX, UK*

<sup>2</sup>*Department of Applied Mathematics, University of Liverpool, Liverpool, L69 3BX, UK*

*Received 7 August 1998; Revised 10 March 1999; Accepted 8 April 1999*

### ABSTRACT

A suite of 27 short cores, 10 of which have been used for magnetic measurements and four for radiometric dating, provides a framework for reconstructing the processes, patterns and rates of sedimentation in Ponsonby Tarn, a small artificial impoundment created towards the end of the 19th century, close to the Sellafield nuclear reprocessing plant in NW England. Spatial and temporal changes in sedimentation are reconstructed and evidence presented for non-synchronicity in magnetic property changes from core to core in the upper part of the sequence, as a result of sorting and selective deposition at different distances from the inflow to the Tarn. Magnetic measurements alone are therefore not a secure basis upon which to quantify sediment yield for defined time intervals at this site. The chronology, established mainly from <sup>210</sup>Pb and <sup>134</sup>Cs analyses, allows estimates of mean sediment yield per annum for four periods: prior to AD 1940, 1940–1964, 1964–1986 and 1986–1991. The rates of sediment accumulation have increased in recent times, especially since 1964, with evidence for input from both magnetically enhanced soils and gleyed alluvial and/or podsolized subsoil sources. Pre-1940 mean annual deposition within the present area of the lake is calculated as 19.5 t a<sup>-1</sup> and for the period since 1986 (the period of maximum sedimentation rates), as 111.3 t a<sup>-1</sup>. These represent yields of 7.0 t km<sup>-2</sup> a<sup>-1</sup> and 39.8 t km<sup>-2</sup> a<sup>-1</sup>, respectively, for the catchment as a whole. Rock magnetic evidence, based on measurements of both bulk samples and the finest particle size separates, suggests that bacterial magnetite, formed within the lake, contributes to the magnetic properties of the sediments, thus modifying the signatures relating to allochthonous sediment input. Copyright © 1999 John Wiley & Sons, Ltd.

KEY WORDS: lake sediments; sediment yields; environmental magnetism; radioisotope dating; <sup>210</sup>Pb; bacterial magnetite

### INTRODUCTION AND SITE DESCRIPTION

The research reported here formed part of a study of the sediments of Ponsonby Tarn commissioned by British Nuclear Fuels Limited (BNFL) and carried out between 1991 and 1993. The primary aims of the study were to identify the spatial and temporal pattern of radionuclides present in the recent sediments and to select cores for further, more detailed investigations relating to the history of atmospheric discharges from the Sellafield nuclear reprocessing plant which lies just 1.5 km to the west of the Tarn. As part of the study, 27 short cores were taken using a Mackereth Minicorer (Mackereth, 1969) and this paper presents the results of magnetic, radiometric, particle-size and loss-on-ignition measurements carried out on some of these cores.

Ponsonby Tarn (National Grid Reference NY046045) lies 3 km from the Irish Sea coast on the southwestern edge of the mountains of the English Lake District, at the junction between the uplands and the narrow coastal plain. It was constructed around AD 1890 by damming the Newmill Beck (Figure 1). The bedrock of the area, comprising Permian and Triassic sandstones, is largely overlain by Late Quaternary fluvioglacial and alluvial materials and the Tarn itself is underlain by Holocene river alluvium. Much of the immediate catchment of the Tarn is covered by managed woodland, though the Newmill Beck has a partly upland catchment covered largely by pasture.

---

\* Correspondence to: Professor F. Oldfield, IGBP Past Global Changes (PAGES) International Project Office, Bärenplatz 2, CH 3011, Bern, Switzerland  
Contract/grant sponsor: British Nuclear Fuels Limited

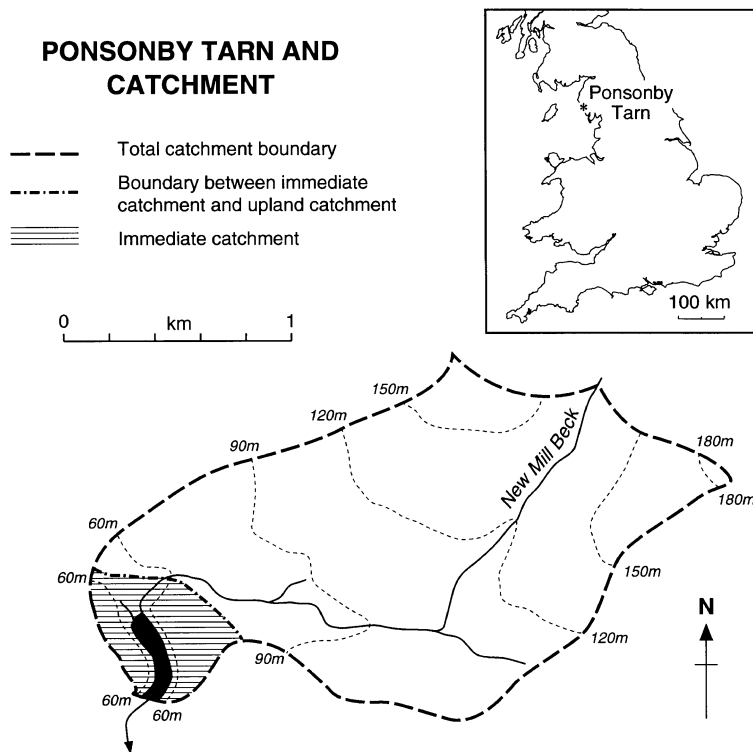


Figure 1. Ponsonby Tarn and its catchment with a site location map (inset). See text for a discussion of the definition of the catchment

The Tarn lies some 50 m above mean sea level and has a surface area of  $0.02 \text{ km}^2$ . It is shallow throughout, with a maximum water depth of 2.5 m close to the dam wall. Its catchment is not easy to define because it lies within an area of rather chaotic, glacially diverted drainage. We have, therefore, defined two components of the catchment, an 'immediate catchment', more or less corresponding with that defined by Bonnett and Cambray (1991) and excluding the area upstream from the swamp at the head to the lake, and a 'total catchment' including both this proximal area and the full drainage basin of the Newmill Beck (Figure 1). Whereas the former has a surface area of only  $0.25 \text{ km}^2$  (cf. Bonnett and Cambray's estimate of  $0.3 \text{ km}^2$ ), the total catchment covers some  $2.8 \text{ km}^2$ .

Earlier studies on the sediments of the Tarn are summarized in Bonnett and Cambray (1991). They mostly comprise analyses of actinide activities within cores taken at various times from 1980 onwards.

### FIELD WORK

Coring was carried out in May 1991. Of the 29 sites where coring was attempted, (Figure 2) only two failed to contain sufficient penetrable material for successful core retrieval. Most of the cores were taken from transect lines defined by roping from bank to bank. All the core locations, as well as the outline of the Tarn, were surveyed with the help of Dr R. Dackcombe, University of Wolverhampton, using an electronic distance meter.

Most of the cores penetrated either the underlying soil or a compact silty sand interpreted as an immediately post-construction deposit, so the results are believed to provide a virtually complete record of sedimentation since the creation of the impoundment. All the cores were described on site and scanned in the field using a Bartington susceptibility meter coupled to a 7.2 cm ID core loop sensor. The traces obtained (Figure 3) and the field notes provided the initial basis for core comparison and for the choice of cores for

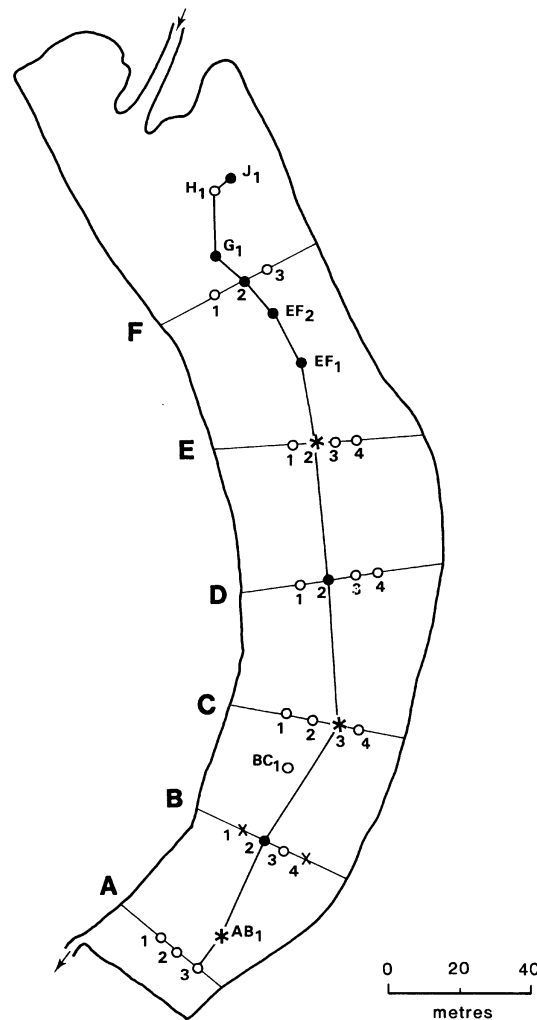


Figure 2. Core sites and roped transect lines used during coring, May 1991. Solid circles mark cores extruded and subsampled for magnetic measurements. Cores marked with an asterisk are those also used for radiometric analysis. Core sites marked with a cross represent points where there was too little sediment to permit successful coring. Empty circles represent successful core sites where the sediments were not extruded and subsampled for measurement. All core sites and the shoreline of the Tarn were surveyed by Dr R. Dackcombe using an electronic distance meter

extrusion and more detailed study. Although the susceptibility traces were useful for core comparison within limited areas of the lake, they failed to provide a correlation scheme for the lake as a whole, partly because of the extent to which they were affected by differences in water content and partly for reasons explored later in interpreting the magnetic measurements subsequently carried out on the subsampled cores.

### LABORATORY METHODS

The 10 cores identified on Figure 2 were chosen for extrusion and subsampling at 1 cm intervals with the exception of EF<sub>1</sub>, which was extruded at 2 cm intervals. Each extruded slice was dried at 40°C and weighed to determine the dry bulk density.

Loss-on-Ignition measurements were carried out on individual subsamples from cores G<sub>1</sub>, EF<sub>1</sub> and E<sub>2</sub> (Figure 4) by combusting 4–5 g of sediment at 450°C for 4 h.

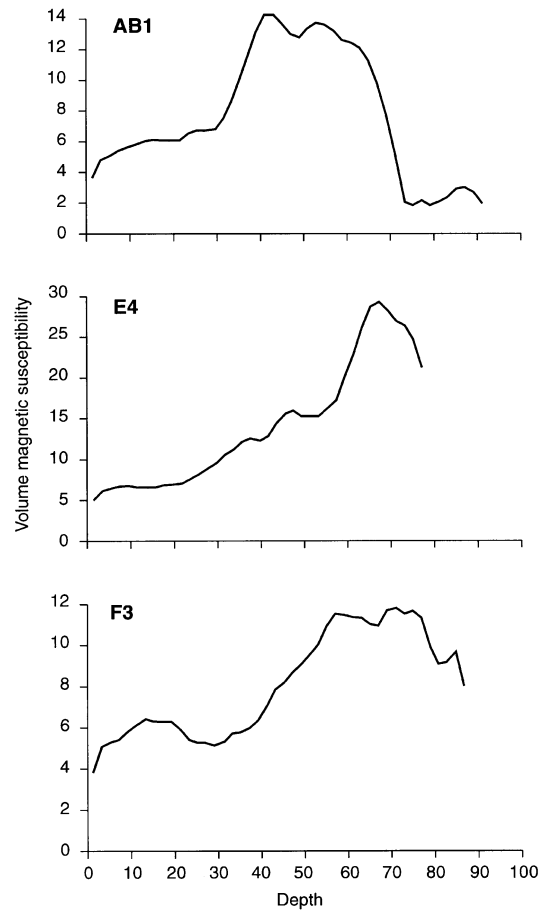


Figure 3. Representative whole-core susceptibility scans carried out in the field. Comparison between the trace for AB<sub>1</sub> and the magnetic measurements for dried subsamples from the same core (Figure 8) show how strongly the susceptibility traces in the upper part of the core are influenced by increasing water content

Particle size analysis was carried out on subsamples from cores G<sub>1</sub>, EF<sub>1</sub> and E<sub>2</sub>, by combining contiguous samples in the depth intervals shown in Figure 5. The procedure used followed Folk (1965) and involved wet-sieving for grades above 62.5  $\mu\text{m}$  and pipetting for finer grades (cf. Oldfield and Yu, 1994).

1. Disaggregated bulk samples were weighed into 100 ml beakers and dispersed ultrasonically with 25 cm<sup>3</sup> calgon (3.3 per cent sodium hexametaphosphate, 0.7 per cent sodium carbonate w/v) and 25 ml deionized water.
2. Each dispersed sample was wet-sieved and the coarser material retained was washed, transferred to beakers and dried at 40°C. This coarser material was then passed through a nest of sieves.
3. Finer grades were separated by pipetting using 500 ml settling cylinders filled with deionized water, shaken end-over-end and placed in a constant temperature (25°C) water bath. A 20 ml sample of the suspension was then pipetted from the cylinder using settling times determined by Stokes law. The weight of each fraction was then determined.

Mass-specific magnetic measurements were generally carried out on alternate samples where 1 cm intervals had been used, but on all samples in the case of cores B<sub>2</sub> and EF<sub>1</sub>. All dried subsamples for magnetic measurement were weighed into clean 10 ml styrene pots and bedded down using cling-film in order to preclude particle movement during measurement.

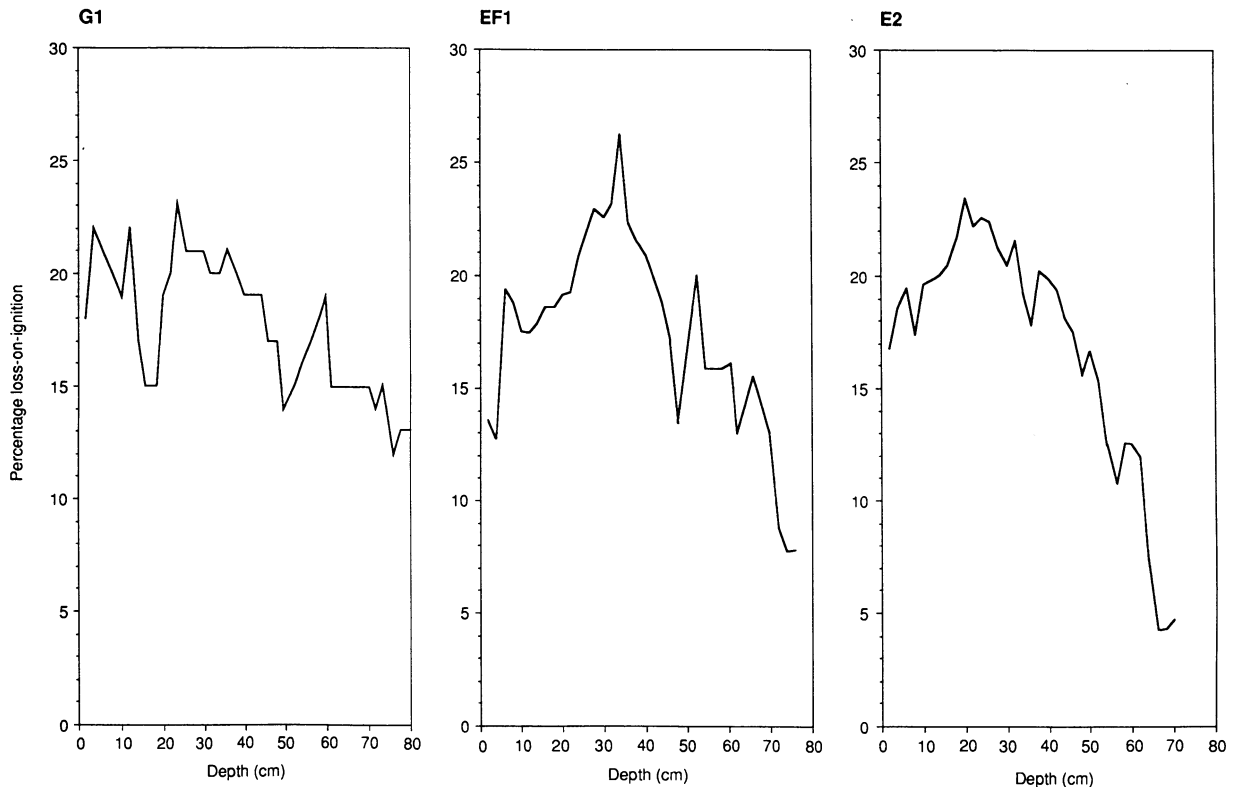


Figure 4. Percentage weight loss on ignition (LOI) for subsamples from three cores spanning the upper to middle reaches of the Tarn

The procedures for magnetic measurement were as summarized in Oldfield and Yu (1994) which also includes an appendix on the interpretation of the magnetic measurements and the quotients and percentage values derived from them. Only in the case of core B<sub>2</sub> was a full suite of magnetic measurements carried out. Measurements on samples from the other cores were limited to anhysteretic remanent magnetization (ARM), plotted here as the susceptibility of ARM ( $\chi_{\text{arm}}$ , a value obtained by normalizing the ARM measurements by the strength of the DC bias field), and isothermal remanent magnetization in forward fields of 20 mT, 300 mT and 1 T (= SIRM). Figure 6 plots the results of the full suite of measurements for core B<sub>2</sub> and Figure 7 plots SIRM,  $\chi_{\text{arm}}$  and  $\chi_{\text{arm}}/\text{SIRM}$  for the remainder of the cores. The first two properties give some indication of the changing concentrations of magnetic minerals within and between each of the cores, whereas the quotient is especially sensitive to changes in *magnetic* grain size, with higher values indicating finer grains. Numbers shown against the  $\chi_{\text{arm}}$  trace in each profile indicate levels where, on the basis of the magnetic properties alone, there would appear to be a basis for correlating the cores (see Figure 12).

Two cores, G<sub>1</sub> and E<sub>2</sub>, were chosen for a more detailed analysis of the relationship between magnetic properties and particle size (Figures 8 and 9). In both cases, subsamples were combined according to the depth intervals shown in the diagrams in order, wherever possible, to provide enough bulk in each size fraction for a full suite of magnetic measurements. The particle size separation was carried out using the methods described above, and the sequence of magnetic measurements followed that in Oldfield and Yu (1994).

Radiometric measurements were carried out on samples from cores EF<sub>2</sub>, D<sub>2</sub>, C<sub>3</sub> and AB<sub>1</sub>. <sup>210</sup>Pb, <sup>226</sup>Ra, <sup>137</sup>Cs, <sup>134</sup>Cs and <sup>241</sup>Am activities were determined by gamma spectrometry using a well-type coaxial, low-background intrinsic germanium detector fitted with a NaI (T1) escape suppression shield (Appleby *et al.*, 1986). Here we present the <sup>210</sup>Pb chronologies calculated using the CRS dating model (Appleby and Oldfield,

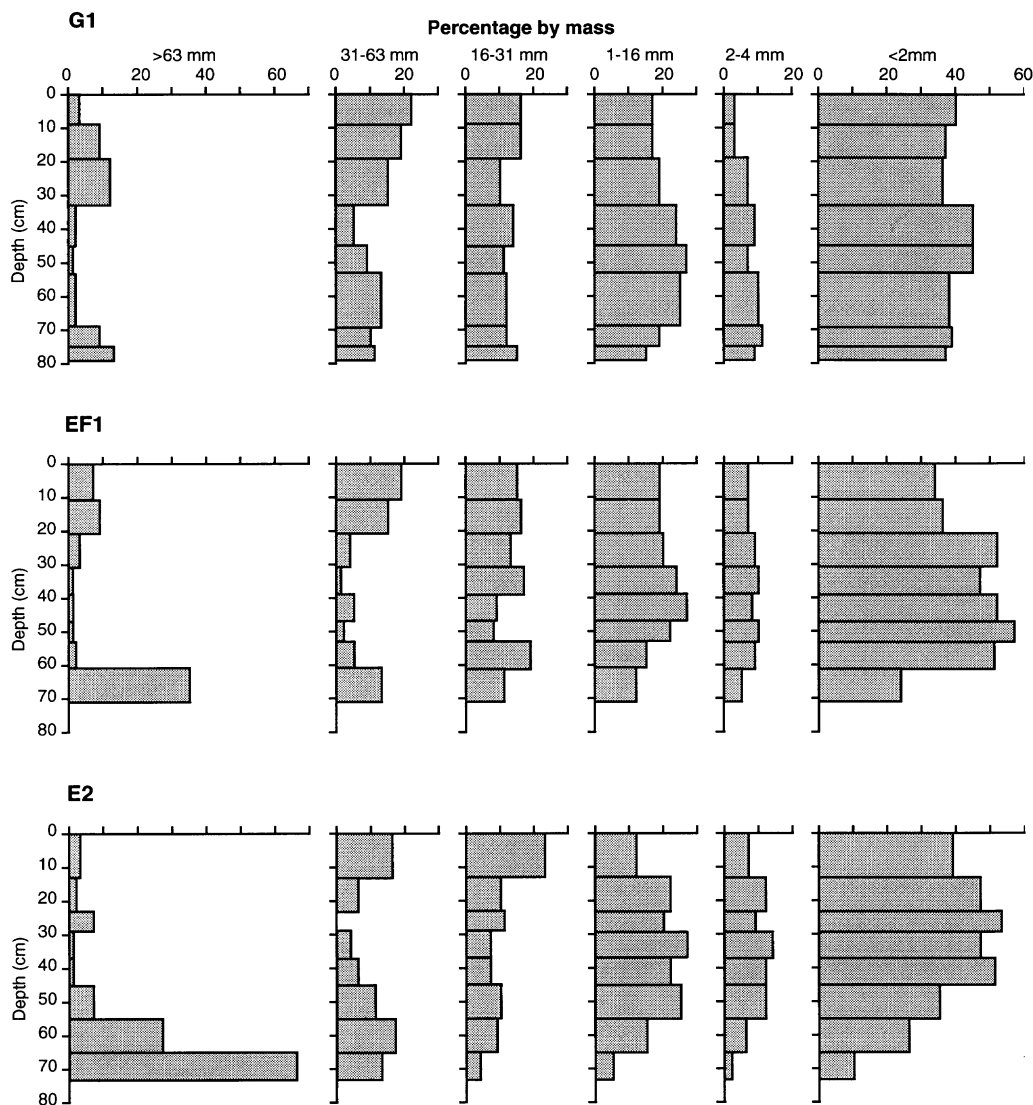


Figure 5. The results of particle-size analysis on combined samples from the three cores also used for LOI determinations (see Figure 4). Each histogram records the percentage of total sample mass falling within the size ranges defined

1978) in Figure 10, the plots of Chernobyl-derived  $^{134}\text{Cs}$  in Figure 11 and the depths at which  $^{241}\text{Am}$  activity exceeds  $0.1 \text{ pCi g}^{-1}$  in Figure 12.

### SEDIMENT CHARACTERISTICS

Loss-on-ignition (LOI) values range from 4 to 27 per cent (Figure 4), with the lowest values reflecting the basal silty sands and pre-reservoir material in cores EF<sub>1</sub> and E<sub>2</sub>. Most values for the sediments proper lie between 15 and 20 per cent. Visual inspection of the cores suggests that a significant proportion of the organic matter is allochthonous, detrital material derived from the catchment, which includes coniferous forests. The calculations of sediment yield made later in the paper have therefore not been adjusted for organic matter content.

Figure 5 shows clear within- and between-core variations in particle size assemblages. The importance of sand-size grades at the base of cores EF<sub>1</sub> and E<sub>2</sub> reflects the nature of the basal inorganic material lying

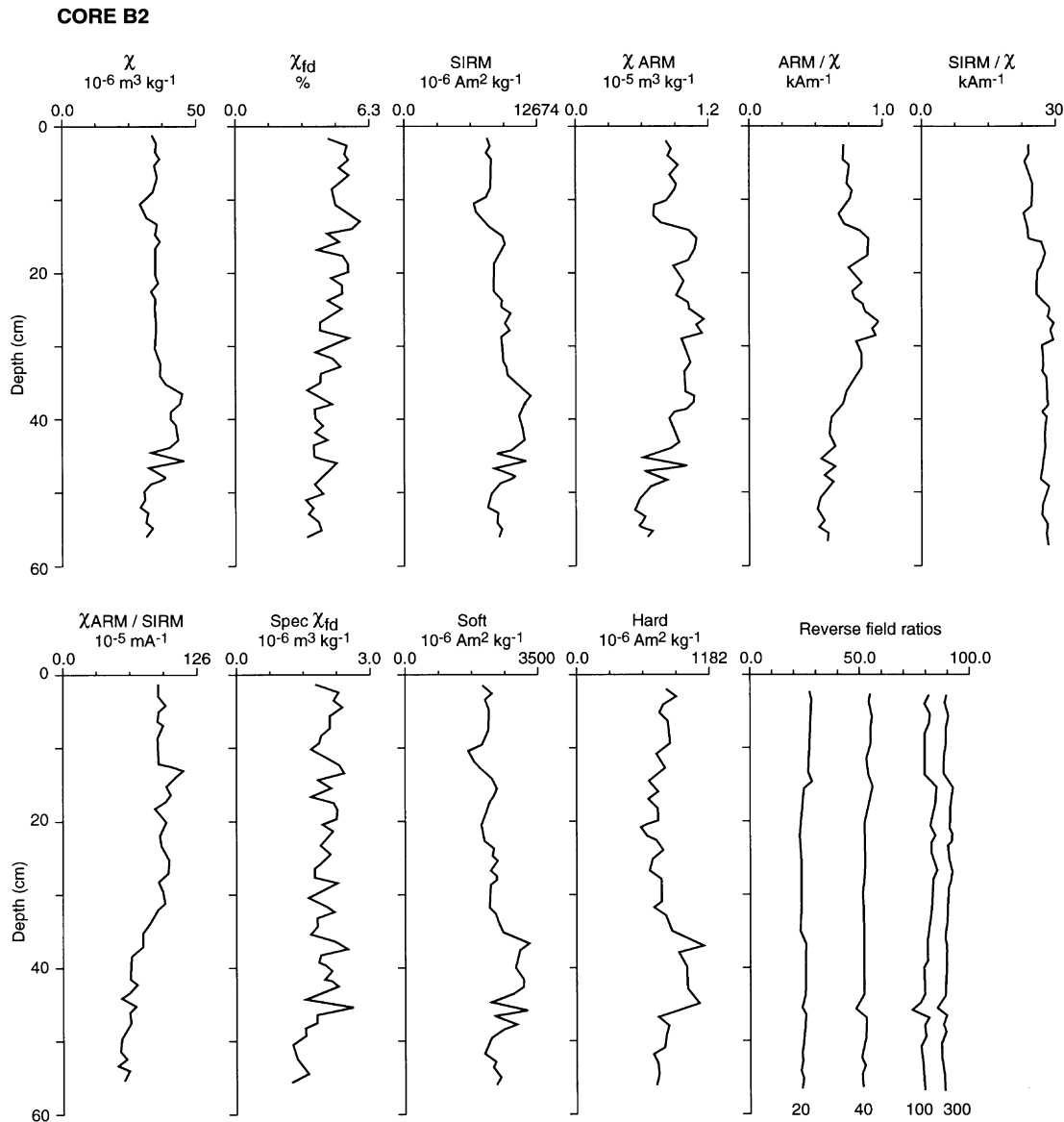


Figure 6. Magnetic measurements for contiguous subsamples at 1 cm intervals from core B<sub>2</sub>. The methods used, the properties measured and the quotients and percentage values derived from them are fully discussed in Oldfield and Yu (1994) and in Chen *et al.* (1995), as are their interpretation

immediately above the soil layer in each core and represents the initial period of sedimentation. Above this, particle sizes in each core are dominated by clay-size ( $<2 \mu\text{m}$ ) material, with cores EF<sub>1</sub> and E<sub>2</sub> showing higher peak values for the finest grade than core G<sub>1</sub>. All three cores have minimum sand percentages somewhere between 60 cm and 30 cm, as well as high clay percentages. Changes in granulometry, often involving a return of coarser grades (both sand and coarse silt), are clearly marked at some depth above *c.* 30 cm in each core. This feature is most strongly in evidence in core G<sub>1</sub>, the one closest to the inflowing stream, with peak sand percentages above 10 and peak coarse silt percentages above 20. All three cores show something of an upward-fining trend in the top 20–30 cm, but whereas in the two cores from closer to the inflow this is seen largely as a shift from sand to coarse silt, in core E<sub>2</sub> it also involves a shift to much higher values for medium silt (31–63  $\mu\text{m}$ ) percentages in the topmost sample. These results suggest that some event

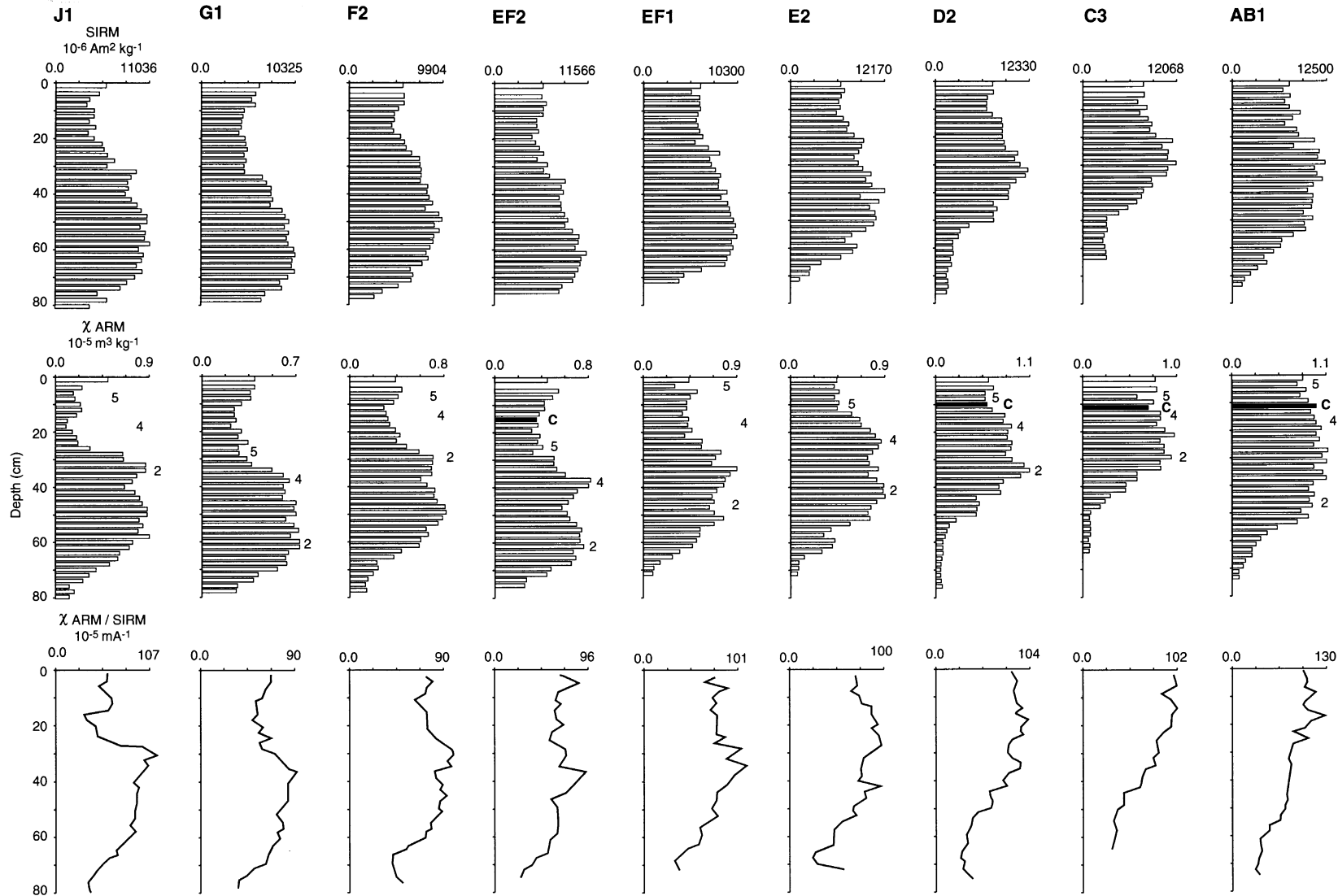


Figure 7. Selected magnetic properties (see text) for cores J<sub>1</sub> to AB<sub>1</sub>. Distances from the inflow increase from left to right (see Figure 2). The numbers 2, 4 and 5 refer to potentially correlatable magnetic horizons. The 'C' to the left of the  $\chi_{\text{ARM}}$  trace in several plots is placed at the depth where peak <sup>134</sup>Cs activity points to the impact of Chernobyl deposition during April/May 1986



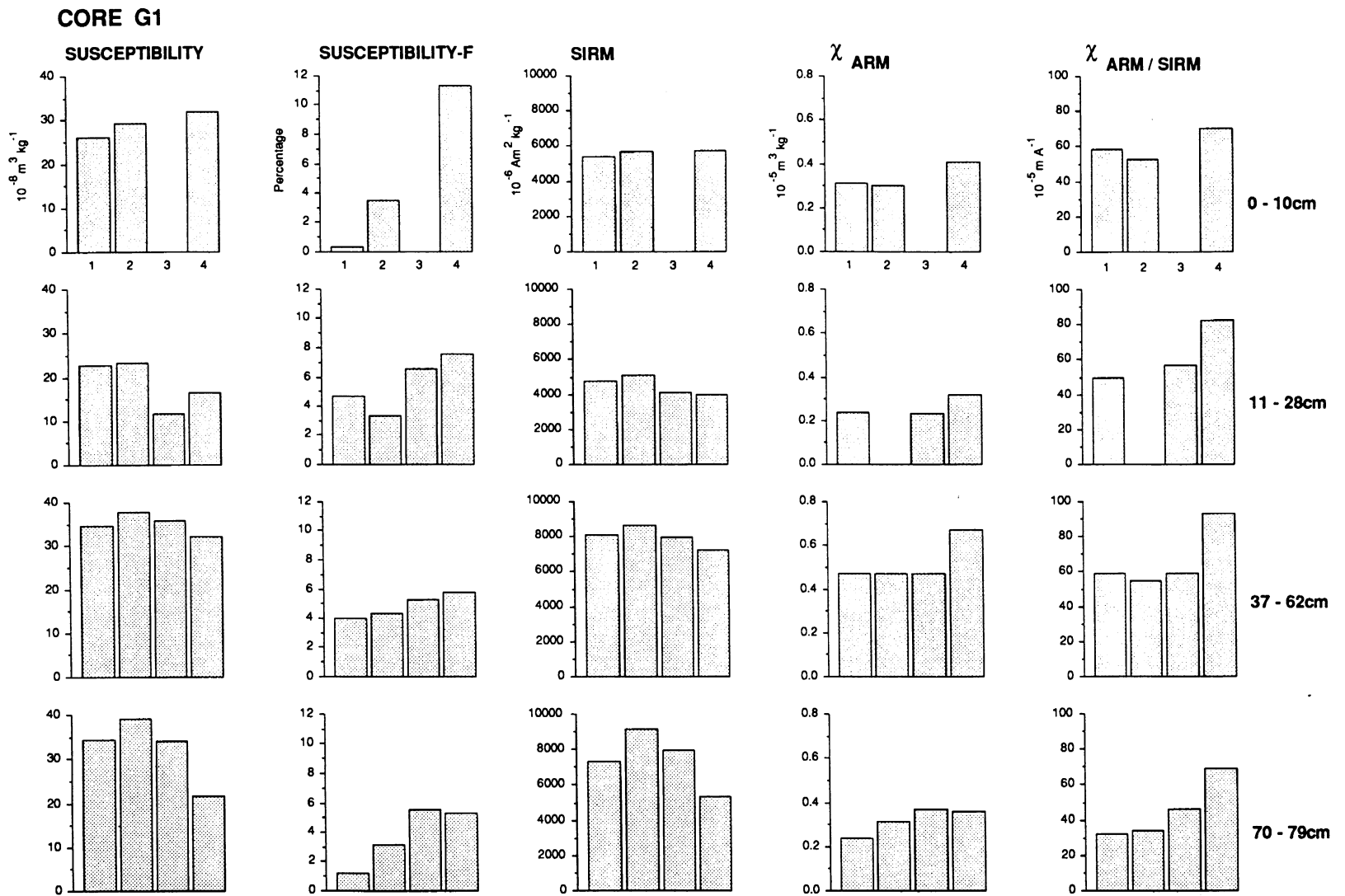


Figure 8. Selected particle-size-based magnetic measurements for combined adjacent subsamples from sections of core G<sub>1</sub>. The histograms plot the magnetic properties for successively finer grades: 1 = > 63  $\mu\text{m}$ , 2 = 31–63  $\mu\text{m}$ , 3 = 2–31  $\mu\text{m}$  and 4 = < 2  $\mu\text{m}$ . Blank columns represent samples accidentally lost or contaminated

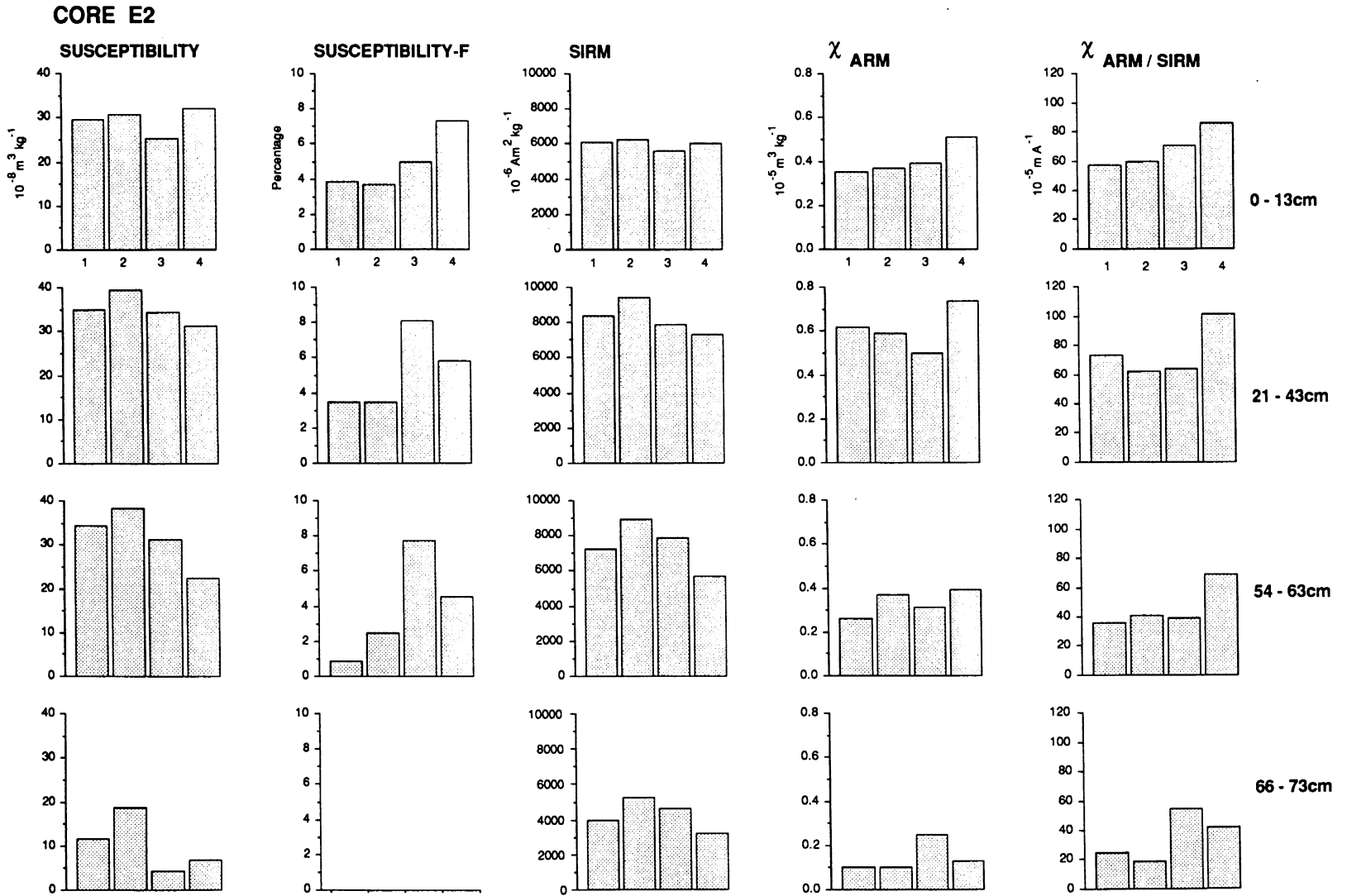


Figure 9. Selected particle-size-based magnetic measurements for combined adjacent subsamples from sections of core E<sub>2</sub>. The histograms plot the magnetic properties for successively finer grades: 1 = > 63  $\mu\text{m}$ , 2 = 31–63  $\mu\text{m}$ , 3 = 2–31  $\mu\text{m}$  and 4 = < 2  $\mu\text{m}$ . Absence of values for  $\chi_{\text{fd}}$  (susceptibility-F) in the lowest sample reflects the unreliability of  $\chi_{\text{fd}}$  measurements on samples with such weak susceptibilities

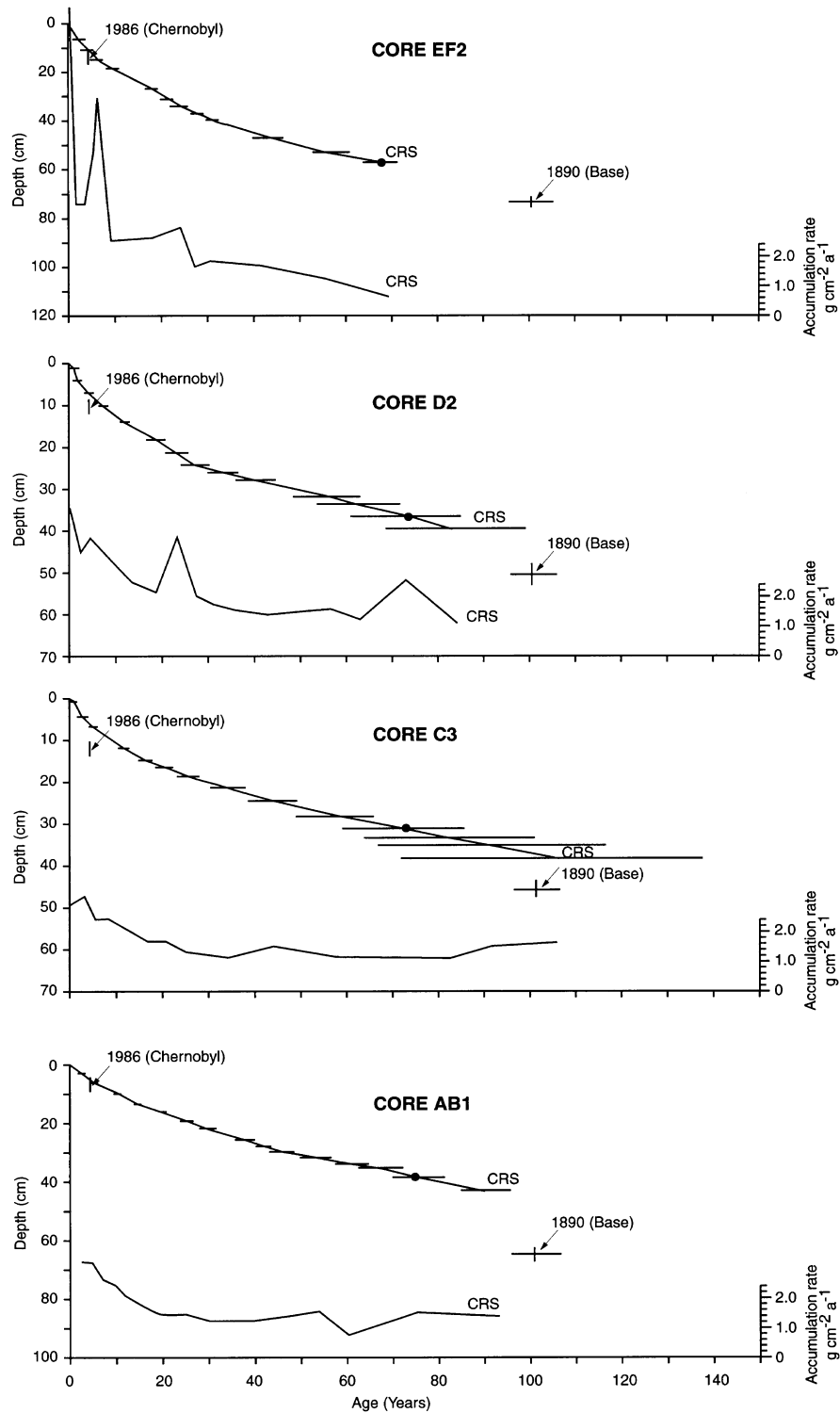


Figure 10. Depth/age curves and dry-mass sediment accumulation rates for each of the radiometrically dated cores, based on treatment of the unsupported  $^{210}\text{Pb}$  values in the manner described in the text. The 1986 Chernobyl horizon (see Figure 12) and the base of fine-grained reservoir sediments are also marked on the plots

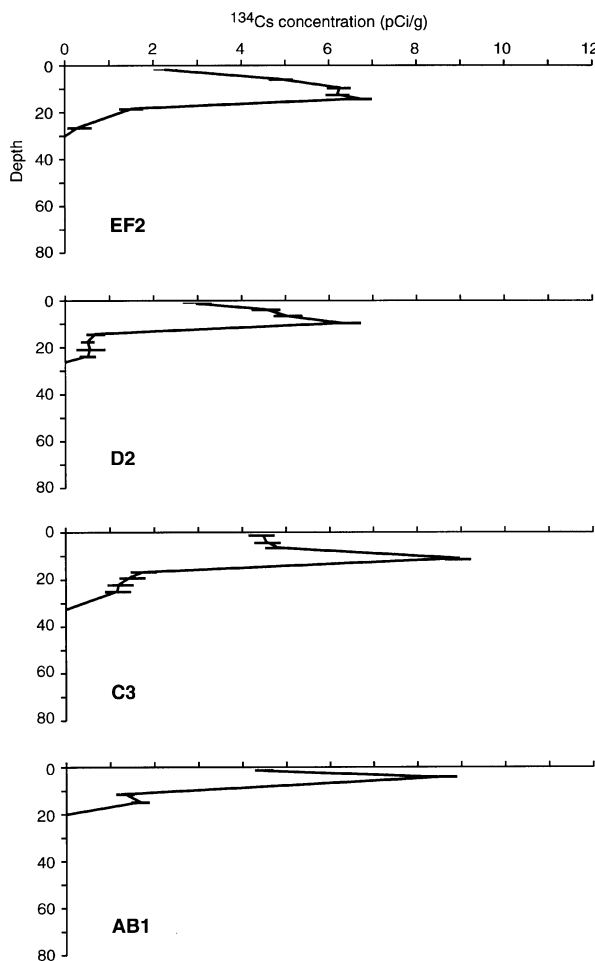


Figure 11. Profiles of  $^{134}\text{Cs}$  activity versus depth for the four cores selected for radiometric analysis. The  $^{134}\text{Cs}$  activities, derived almost exclusively from Chernobyl fallout, have been corrected for decay since May 1986

or land use change in the part of the catchment drained by the Newmill Beck triggered delivery of coarser material to the Tarn and that this material was deposited selectively with the coarser grades sedimenting preferentially in the upper reaches of the Tarn.

Figures 6 and 7, graphing the down-core variations in bulk magnetic properties, and Figures 8 and 9, showing the links between particle size and magnetic characteristics, may be interpreted in part in the light of the above considerations. The minimum magnetic concentrations in the basal samples from E<sub>2</sub>, D<sub>2</sub>, C<sub>3</sub> and AB<sub>1</sub> come from samples of basal sandy silt and underlying soil. The particle-size-based magnetic measurements from the basal material of core E<sub>2</sub> (Figure 9) show that grade-for-grade, this material is less magnetic than the later sediments of the Tarn. This may reflect a difference in source and/or the effects of *in-situ* gleying in the alluvial material underlying the Tarn (cf Maher, 1986).

The magnetic profiles from the upstream cores between the 'E' line and the inflow (Figure 7) all show lower magnetic concentrations in the more recent sediments. This decline towards the surface is much less marked in the cores closer to the dam wall. The minimum values for SIRM and  $\chi_{\text{arm}}$  are lower and at greater depth in the 'upstream' than in the 'downstream' cores. Comparison between the bulk magnetic and the particle size (Figure 5) profiles shows a clear link between the levels with coarser grades and those with lower magnetic concentrations. In the case of  $\chi_{\text{arm}}$ , this may be partly explained by the way in which, as in many other cases (e.g. Zheng *et al.*, 1991; Yu and Oldfield, 1993; Oldfield and Yu, 1994; Chen *et al.*, 1995), values

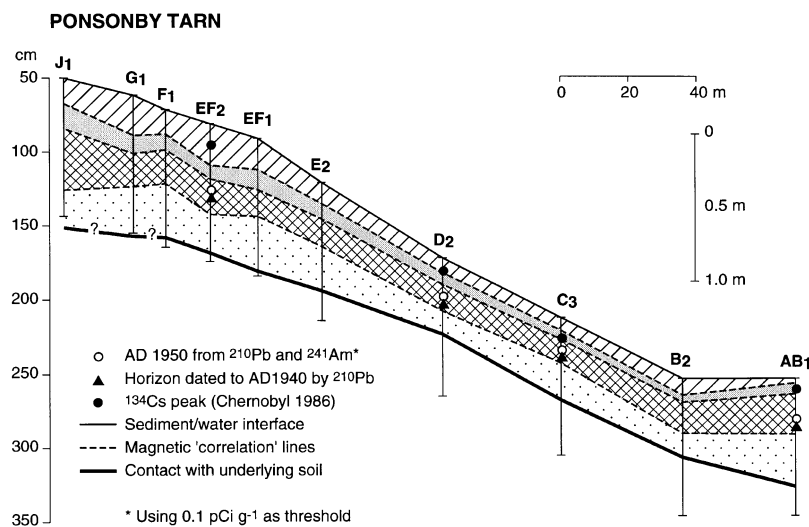


Figure 12. Magnetic subdivisions of all the cores subsampled, using the horizons defined on Figures 7. Each core is plotted at the correct relative water depth and the distances between cores are proportional to their actual distances apart. Two radiometric dates have been superimposed on the appropriate plots. The lower one is based on a good agreement between the depth dated by  $^{210}\text{Pb}$  as AD 1950 and the point in the  $^{241}\text{Am}$  profiles at which values rise above  $0.1 \text{ pCi g}^{-1}$ . The upper one is taken from the peaks in Chernobyl-derived  $^{134}\text{Cs}$  activity recorded in Figure 11. Whereas the lower magnetic subdivisions are compatible with the earlier date, the upper ones are shown to be non-synchronous

for this property are higher in the finer than in the coarser grades (Figures 8 and 9). The same explanation does not serve for the reduction in SIRM values in core  $G_1$ . Within any given grade, the SIRM values decline up-core by around 40 per cent. This can be clearly seen by comparing the values for the composite sample from 37–62 cm with those for the sample from 11–28 cm. There is no link between particle size and SIRM values that would permit an interpretation of the up-core decline solely in terms of the changes in particle size proportions. It is therefore necessary to invoke some shift to a less magnetic sediment source type in addition to the coarsening of the particle size assemblage. One possibility might be an increase in the proportion of unweathered material, since the local bedrock and the glaciofluvial materials derived from it are rich in haematite. This interpretation is not supported by the 'hard' IRM values, shown here only for core B2 (Figure 6) which do not vary systematically either within or between cores and consistently show values close to 10 per cent of the total SIRM. An increased input of relatively coarse, somewhat gleyed, within-valley alluvial material and/or podsolized subsoil material is inferred. Both source types would be likely to yield material magnetically depleted in all particle sizes (Maher, 1986). There is evidence for both channel excavation and for the clear felling of areas of former conifer plantation in the catchment; these processes may have been responsible for the upward shift towards sediments that are less magnetic, grade for grade, in the cores close to the inflow.

Although the down-profile changes in magnetic properties are not explicable in terms of changing grade alone, some of the changes in magnetic properties between profiles may be related to the temporal and spatial shifts in particle size proportions already discussed. The downstream increase in minimum  $\chi_{\text{arm}}$  values already noted is accompanied by a similar increase in the peak values for  $\chi_{\text{arm}}/\text{SIRM}$  in each core. Setting aside a single anomalous peak value in  $J_1$ , the trend is as follows:  $G_1$ –89;  $F_2$ –91;  $EF_2$ –97;  $EF_1$ –101;  $E_2$ –101;  $D_2$ –104;  $C_3$ –102;  $B_2$ –127;  $AB_1$ –131. Such an almost perfectly consistent downstream trend indicates a gradual shift in mean magnetic grain size, with the finest grains becoming increasingly important away from the inflow. All the values are consistent with a magnetic mineral assemblage dominated by stable single domain grains (cf. Maher, 1988) with diameters between  $0.1 \mu\text{m}$  and  $0.02 \mu\text{m}$ , which, in turn, is consistent with the dominance of clay-size particles in the sediments. This, as well as the clear link to particle size shown by the  $\chi_{\text{fd}}\%$  values (Figures 8 and 9) is discussed further in a subsequent section evaluating the possibility of both magnetically enhanced soil and bacterial contributions to the magnetic record.

## THE CHRONOLOGY OF SEDIMENTATION

Because of the highly non-monotonic nature of the unsupported  $^{210}\text{Pb}$  concentration profiles, calculation of dates using the CIC  $^{210}\text{Pb}$  dating model (Appleby and Oldfield, 1978), was not feasible. In calculating the chronologies shown in Figure 10, the age/depth curves have been constrained at the base by using the depth at which activity has declined to  $0.5 \text{ pCi g}^{-1}$  as representing *c.* AD 1917. Since surficial concentrations of unsupported  $^{210}\text{Pb}$  are similar in all four cores, it seems reasonable to suppose that this level of activity may also denote a synchronous horizon. The depth at which it occurs can be clearly identified in three of the four cores, though less easily in EF<sub>2</sub>. Such a procedure avoids attempting to deal with any possible disturbance of the  $^{210}\text{Pb}$  record during the initial phase of sedimentation following the creation of the Tarn around AD 1890. The date of AD 1917 for the constraining horizon was arrived at by an iterative procedure based on the 'correlated CRS'  $^{210}\text{Pb}$  dating model described in Oldfield *et al.* (1980), using as correlating features, the well identified peaks in Chernobyl-derived  $^{134}\text{Cs}$  activity (Figure 11), the  $1.0$  and  $0.5 \text{ pCi g}^{-1}$  unsupported  $^{210}\text{Pb}$  levels, and the basal level indicated by the abrupt increase in sediment bulk density. In order to minimize the use of possibly contentious assumptions, the chronologies shown in Figure 10 have not made use of correlation features other than the  $0.5 \text{ pCi g}^{-1}$  level, though the differences between the chronologies used and those derived from the 'correlated CRS' model are negligible.

The  $^{210}\text{Pb}$  dates for cores D<sub>2</sub>, C<sub>3</sub> and AB<sub>1</sub> all indicate a period of slow, consistent sedimentation from *c.* AD 1910 into the 1950s, followed by a dramatic increase in accumulation rates. Comparison with the levels at which peak deposition of  $^{134}\text{Cs}$  occurs, resulting from the Chernobyl accident in 1986, suggests that the  $^{210}\text{Pb}$  dates may actually underestimate this recent acceleration. The chronology may be less secure in the case of core EF<sub>2</sub>, since there is almost no systematic decline in unsupported  $^{210}\text{Pb}$  in the top 57 cm, below which there is an abrupt transition to equilibrium values at 60 cm. This evidence alone might point to a gap in sedimentation at the site, but the magnetic record tends not to support such an inference, since the core contains a good record of the features represented in other cores from nearby. A dramatic increase in sedimentation rate between 57 and 60 cm is inferred.

## ESTIMATED SEDIMENT YIELDS

As a first stage in calculating sediment yields for parts of the period of sedimentation, Figure 12 has been compiled from the magnetic profiles and the radiometric chronology. It uses the three 'correlating' features in Figures 6–8 along with the base of reservoir sedimentation to define four 'zones' of sedimentation in each core. Onto these are superimposed dated horizons from the  $^{210}\text{Pb}$ - and  $^{134}\text{Cs}$ -derived chronology. Whereas the magnetically defined 'zones' are consistent with the chronological horizons for the period up to *c.* AD 1950, the upper horizons are not consistent with the 1986 Chernobyl spike. This demonstrable non-synchronicity of magnetic features is also illustrated in Figures 7 and 8 and is best explained by the sorting and depositional processes already inferred from the particle size and magnetic results. The latter show clear signs of sorting with distance from in-flowing stream as well as a link between some magnetic properties, notably  $\chi_{\text{arm}}$  and  $\chi_{\text{arm}}/\text{SIRM}$ , and particle size. This has given rise to a downstream facies change in magnetic properties that makes the magnetostratigraphic 'correlations' non-synchronous. In the present case, therefore, using magnetic measurements alone does not give a valid basis for reconstructing total sedimentation in the Tarn.

In reconstructing sediment yields, four dated horizons have been used: AD 1940 and 1964, both of which seem well correlated between cores in a way consistent with the magnetic profiles; 1986 derived from the Chernobyl spike; and the sediment surface retrieved during coring in 1991. This allows four time intervals to be defined: pre-1940, 1940–1964, 1964–1986 and 1986–1991. Mean annual dry-mass sedimentation can be determined from the radiometric chronologies and the cumulative dry bulk density measurements used in their calculation. For the period before 1940, in view of uncertainties about core chronology in the earlier and probably unrepresentative stages of infill, we have calculated mean annual rates only for the parts of the  $^{210}\text{Pb}$  profiles dating from *c.* AD 1917 to 1940.

The accumulation rates, once determined, have been used to provide estimates of total sedimentation within the Tarn assuming that the mean rate of all four cores will be a reasonable approximation of the mean

Table I. Mean sedimentation rates and sediment yields

|  | pre-1940 | 1940–1964 | 1964–1986 | 1986–1991 |
|--|----------|-----------|-----------|-----------|
| (A) Mean sedimentation rates in each dated core ( $\text{g cm}^{-2} \text{ a}^{-1}$ )                                  |          |           |           |           |
| EF <sub>1</sub>  | 0.11     | 0.17      | 0.27      | 1.06      |
| D <sub>2</sub>   | 0.09     | 0.09      | 0.20      | 0.41      |
| C <sub>3</sub>   | 0.08     | 0.08      | 0.07      | 0.37      |
| AB <sub>1</sub>  | 0.10     | 0.11      | 0.14      | 0.44      |
| Mean rates for all four cores  | 0.10     | 0.11      | 0.17      | 0.57      |
| (B) Calculated mean annual sediment yields ( $\text{t a}^{-1}$ )   |          |           |           |           |
|  | 19.5     | 21.5      | 33.2      | 111.3     |
| (C) Mean annual yield per $\text{km}^2$ of 'immediate' catchment (see Figure 1) ( $\text{t km}^{-2} \text{ a}^{-1}$ )> |          |           |           |           |
|  | 78       | 86        | 133       | 445       |
| (D) Mean annual yield per $\text{km}^2$ of whole catchment (see Figure 1) ( $\text{t km}^{-2} \text{ a}^{-1}$ )        |          |           |           |           |
|  | 7.0      | 7.7       | 11.9      | 39.8      |

rate in the Tarn as a whole, and using a figure of  $19\,500 \text{ m}^2$  as the area over which sediments have accumulated within the Tarn. This figure includes 75 per cent of the bed of the Tarn (estimated from the total area over which initial probing indicated that sediments were distributed), plus  $4500 \text{ m}^2$ , the approximate surface area covered by recently developed reedswamp at the head of the lake. The various calculations and assumptions used, together with the areas of the 'immediate' and 'total' catchment already noted, permit the estimates summarized in Table I. The high sedimentation rates during the 1980s may be a response to the effects of clear-felling close to the eastern shore of the Tarn as reported by E.Y. Haworth and noted in Bonnett and Cambray (1991). Comparison with the results summarized in Foster (1995) shows that the calculated values are reasonably compatible with those for Merevale lake in the English Midlands, the catchment of which has land use similar to that in the immediate catchment of Ponsonby Tarn. The values are significantly lower than the peak yields noted by Foster for Seeswood Pool, another Midland site, and for Slapton Ley on the south coast of England, both of which include extensive cultivated areas.

#### SEDIMENT SOURCES AND THE QUESTION OF BACTERIAL MAGNETITE

Recent studies of Lake District lakes (Van der Post *et al.*, 1997; Oldfield and Wu, in press) have shown systematic differences in the magnetic properties of the finest grained material in the sediments and the pedogenically altered material in the catchments from which the allochthonous fines must have been derived. In the case of both Blelham Tarn and Brothers Water, lakes with relatively more lowland and upland catchments respectively, it was suggested that a bacterial contribution to the magnetic properties of the sediment was detectable. This contribution, in the form of biosynthesized 'magnetosomes' was inferred from the demonstration that the offset in magnetic properties between the finest catchment and sediment samples was best explained by an additional input of stable single domain (SSD) magnetite grains to the latter. Bacterial magnetosomes have been detected by means of high resolution transmission electron microscopy (HRTEM) in a wide range of sites (e.g. Vali *et al.*, 1987; Chang *et al.*, 1989) and their contribution to the record in the Ponsonby Tarn sediments cannot be precluded. This possibility has been explored using rock magnetic evidence alone, since access to HRTEM was not available.

Oldfield (1994) proposed a basis for identifying a bacterial magnetosome contribution to the magnetic record using a bilogarithmic plot of  $\chi_{\text{arm}}/\chi$  and  $\chi_{\text{arm}}/\chi_{\text{fd}}$ . Provided the samples used for calculation of the quotients are first carefully screened to ensure that they are dominated by SSD grains or finer, using the criteria set out in Oldfield (1994), low values for these quotients indicate magnetic grain size assemblages rich in sub-SSD sizes (predominantly superparamagnetic). High values point to exclusively SSD assemblages. The former are typical of magnetically enhanced (cf. Mullins, 1977; Dearing *et al.*, 1996a,

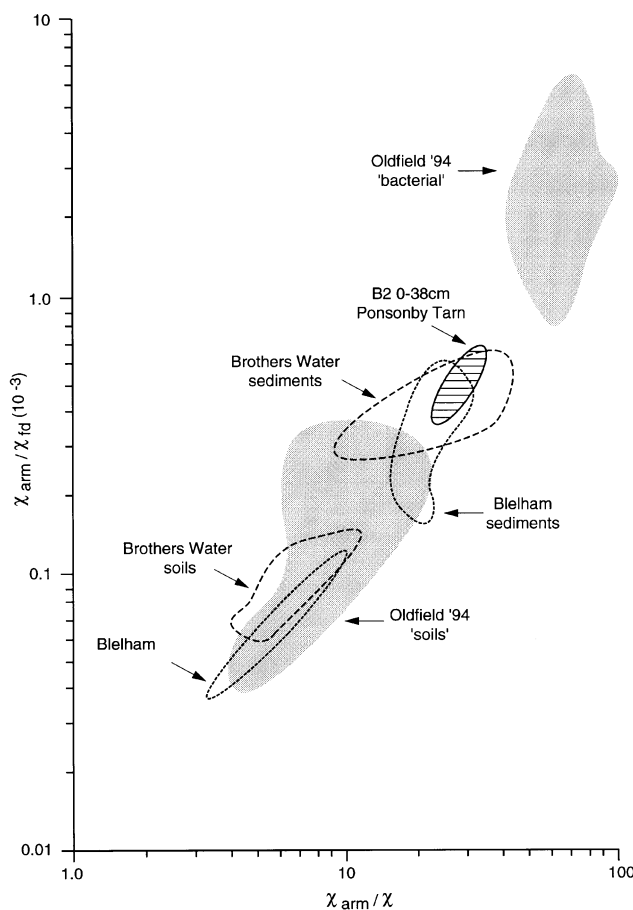


Figure 13. Bilogarithmic plots of  $\chi_{\text{arm}}/\chi$  versus  $\chi_{\text{arm}}/\chi_{\text{fd}}$  (see Oldfield, 1994) onto which are superimposed envelopes of values for 'soils' and sediments from a range of other sites. The values for Blenheim Tarn are from Van der Post *et al.* (1997) and those for Brothers Water from Oldfield and Wu (in press). The interpretation of the plot is considered in the text

b) soils and of the sediments derived directly and exclusively from them. The latter reflect the size control exercised in biosynthesis to ensure that magnetotaxis is achieved. Figure 13 uses the bilogarithmic plot to compare the values for sediments from the top 38 cm of core B<sub>2</sub> with those used in the original article, as well as those derived from the Blenheim Tarn (Van der Post, 1997) and Brothers Water (Oldfield and Wu, in press) studies. The Ponsonby Tarn samples fall within a very narrow range of values between the 'soil/detrital' and 'bacterial' envelopes in the original article, but well within the envelope of values for Blenheim and Brothers Water sediments. From this, we tentatively conclude that the lateral facies change in magnetic properties demonstrated for the upper part of the Ponsonby Tarn infill may reflect not only sorting, but some deposition of bacterial magnetosomes in the lower reaches of the Tarn.

The finest silt and clay fractions in cores G<sub>1</sub> and E<sub>2</sub> include material with  $\chi_{\text{fd}}\%$  values between 8 and 12. These values are typical of magnetically enhanced soils (Dearing *et al.*, 1996a, b). The particle-size-based magnetic measurements thus give a strong indication of some input of ultra-fine grained, soil-derived 'magnetite' and, as in the case of the two previous studies of Lake District lakes, we conclude that both soil-derived, detrital and *in situ* 'bacterial' material is represented in the fine-grained magnetic minerals in the sediments. In addition to these components in the fine sediment grades, evidence for a recent input of coarse material from gleyed alluvial and/or podsollic subsoil sources has already been noted. The magnetic properties thus reflect a complex mixture related to changes in source types, to particle sorting within the lake itself, and



to what we tentatively interpret here as both spatial and temporal variations in the autochthonous contribution from bacterial magnetite. They appear to offer little scope for any simple quantitative source modelling.

## CONCLUSIONS

1. Despite the shallowness of the Tarn, and perhaps because of its relatively sheltered position, the combined results from magnetic and radiometric measurements indicate reasonably conformable deposition over much of the bed of the Tarn and provide a robust chronological framework for reconstructing sedimentation rates, processes and patterns over the last 70–80 years.
2. During the period since *c.* AD 1960, there has been a strong acceleration in sedimentation over most of the bed of the Tarn. The sediments are predominantly of clay size, though the recent ones are, on average, coarser than those deposited during the preceding decades. These recent sediments have been sorted during transport, with the larger particles preferentially deposited in the upstream parts of the Tarn.
3. This sorting and selective deposition has given rise to small-scale facies changes within the lake, which in turn have meant that not all changes in magnetic properties are synchronous from core to core down the full length of the Tarn in the recent period.
4. The chronology of sedimentation developed from the radiometric measurements makes possible a quantitative reconstruction of the mean annual sediment yield to the lake for the period before AD 1940, and the periods 1940–1964, 1964–1986 and 1986–1991, the year when the cores were taken. The calculations point to a strong acceleration in sedimentation, especially since 1964, with yields for the latest period ( $111.3 \text{ t a}^{-1}$ ) exceeding those for the earliest by a factor of between five and six times. The high sedimentation rates during the 1980s may have resulted from the clear-felling of part of the immediate catchment of the lake reported by E.Y. Haworth and noted in Bonnett and Cambray (1991).
5. The magnetic properties of the Tarn sediments and their predominantly clay size suggest that surface soil erosion may have been a significant source of allochthonous material. There is also some suggestion that gleyed alluvium and/or podsolized subsoils with reduced magnetic concentrations may also have made an important contribution, especially to the post-1960 sediments in the ‘upstream’ part of the Tarn.
6. The finest magnetic grains in the sediment have properties intermediate between those believed to indicate exclusively soil sources and those typical of biogenic magnetite formed within the lake by magnetotactic bacteria. Both are probably represented in the sediments.

## ACKNOWLEDGEMENTS

We are grateful to BNFL for funding the research upon which the results presented here are based, to Jan Bloemendal, Patrick Bonnett and Simon Hutchinson for help with field work, and to Roger Dackcombe for surveying the site and coring operations. Sandra Mather’s assistance in preparing the figures is also gratefully acknowledged.

## REFERENCES

- Appleby, P. G. and Oldfield, F. 1978. ‘The calculation of lead-210 dates assuming a constant rate of supply of unsupported  $^{210}\text{Pb}$  to the sediment’, *Catena*, **5**, 1–8.
- Appleby, P. G., Nolan, P., Gifford, D. W., Godfrey, M. J., Oldfield, F., Andersen, N. J. and Battarbee, R. W. 1986. ‘ $^{210}\text{Pb}$  dating by low background gamma counting’, *Hydrobiologia*, **141**, 21–27.
- Bonnett, P. J. P. and Cambray, R. S. 1991. ‘The record of deposition of radionuclides in the sediments of Ponsonby Tarn, Cumbria’, *Hydrobiologia*, **214**, 63–70.
- Chang, S., Chang, B. R. and Kirschvink, J. L. 1989. ‘Magnetofossils, the magnetization of sediments and the evolution of biomineralization’, *Annual Review of Earth and Planetary Science*, **17**, 169–195.
- Chen, F., Wu, R., Pompei, D. and Oldfield, F. 1995. ‘Magnetic property and particle size variations in the late Pleistocene and Holocene parts of the Dadongling loess section near Xining’, in Derbyshire, E. (Ed.), *Windblown Sediments in the Quaternary Record*, *Quaternary Proceedings*, **4**, 27–40.
- Dearing, J. A., Dann, R. J. L., Hay, K., Lees, J. A., Loveland, P. J., Maher, B. A. and O’Grady, K. 1996a. ‘Frequency-dependent

- susceptibility measurements of environmental materials', *Geophysical Journal International*, **124**, 228–240.
- Dearing, J. A., Hay, K. L., Baban, S. M. J., Huddleston, A. S., Wellington, E. M. H. and Loveland, P. J. 1996b. 'Magnetic susceptibility of soil: an evaluation of conflicting theories using a national data set', *Geophysical Journal International*, **127**, 728–734.
- Folk, R. L. 1965. *Petrology of Sedimentary Rocks*, Hemphill's, Austin, Texas.
- Foster, I. D. L. 1995. 'Lake and reservoir bottom sediments as a source of soil erosion and sediment transport data in the UK', in Foster, I. Gurnell, A. and Webb, B. (Eds), *Sediment and Water Quality in River Catchments*, Wiley, Chichester, 265–283.
- Mackereth, F. J. H. 1969. 'A short core sampler for subaqueous deposits', *Limnology and Oceanography*, **14**, 145–151.
- Maher, B. A. 1986. 'Characterisation of soils by mineral magnetic measurements', *Physics of the Earth and Planetary Interiors*, **42**, 76–92.
- Maher, B. A. 1988. 'Magnetic properties of some synthetic, sub-micron magnetites', *Journal of Geophysical Research*, **94**, 83–96.
- Mullins, C. E. 1977. 'Magnetic susceptibility of the soil and its significance in soil science: a review', *Journal of Soil Science*, **28**, 223–246.
- Oldfield, F. 1994. 'Toward the discrimination of fine-grained ferrimagnets by magnetic measurements in lake and near-shore marine sediments', *Journal of Geophysical Research*, **99**, 9045–9050.
- Oldfield, F. and Wu, R. (in press) 'The magnetic properties of the recent sediments of Brothers Water, N W England', *Journal of Paleolimnology*.
- Oldfield, F. and Yu, L. 1994. 'The influence of particle size variations on the magnetic properties of sediments from the north-eastern Irish Sea', *Sedimentology*, **41**, 1093–1108.
- Oldfield, F., Appleby, P. G. and Thompson, R. 1980. 'Palaeoecological studies of lakes in the highlands of Papua New Guinea. 1. The chronology of sedimentation', *Journal of Ecology*, **68**, 457–477.
- Vali, H., Frster, G., Amarantides, G. and Petersen, N. 1987. 'Magnetotactic bacteria and their magnetofossils in sediments', *Earth and Planetary Science Letters*, **86**, 389–400.
- Van der Post, K. D., Oldfield, F., Haworth, E. Y., Crooks, P. R. J. and Appleby, P. G. 1997. 'A record of accelerated erosion in the recent sediments of Blelham Tarn in the English Lake District', *Journal of Paleolimnology*, **18**, 103–120.
- Yu, L. and Oldfield, F. 1993. 'Quantitative sediment source ascription using magnetic measurements in a reservoir catchment system near Nijar, S.E. Spain', *Earth Surface Processes and Landforms*, **18**, 441–454.
- Zheng, H., Oldfield, F., Yu, L., Shaw, J. and An, Z. 1991. 'The magnetic properties of particle-sized samples from the Luo-Chuan loess section: evidence for pedogenesis', *Physics of the Earth and Planetary Interiors*, **68**, 250–258.